PROTEIN STRUCTURE REPORT

Solution structure of protein synthesis initiation factor 1 from *Pseudomonas aeruginosa*

Yanmei Hu, Alejandra Bernal, James M. Bullard, and Yonghong Zhang*

Department of Chemistry, The University of Texas Rio Grande Valley, Edinburg, Texas

Received 11 July 2016; Accepted 9 September 2016
DOI: 10.1002/pro.3042
Published online 16 September 2016 proteinscience.org

Abstract: *Pseudomonas aeruginosa* is an opportunistic bacterial pathogen and a primary cause of nosocomial infection in humans. The rate of antibiotic resistance in *P. aeruginosa* is increasing worldwide leading to an unmet need for discovery of new chemical compounds distinctly different from present antimicrobials. Protein synthesis is an essential metabolic process and a validated target for the development of new antibiotics. Initiation factor 1 from *P. aeruginosa* (Pa-IF1) is the smallest of the three initiation factors that act to establish the 30S initiation complex during initiation of protein biosynthesis. Here we report the characterization and solution NMR structure of Pa-IF1. Pa-IF1 consists of a five-stranded β-sheet with an unusual extended β-strand at the C-terminus and one short α-helix arranged in the sequential order β1-β2-β3-α1-β4-β5. The structure adopts a typical β-barrel fold and contains an oligomer-binding motif. A cluster of basic residues (K39, R41, K42, K64, R66, R70, and R72) located on the surface of strands β4 and β5 near the short α-helix may compose the binding interface with the 30S subunit.

Keywords: *Pseudomonas aeruginosa*; translation initiation factor 1; β-barrel motif; NMR structure

Introduction

Pseudomonas aeruginosa is a ubiquitous Gram-negative bacterium that is capable of surviving in a broad range of natural environments due to its large metabolic versatility and flexibility. It is an important opportunistic pathogen and a causative agent of both severe acute infections and chronic infections.[1] Recently, multi-drug resistance developed by *P. aeruginosa* strains has become a serious problem.[2] The rate of antibiotic resistance in *P. aeruginosa* is increasing worldwide and this has created the need for new compounds that inhibit growth of the bacteria with a substantially different mode of action and range of molecular targets than current antibiotics.

Protein synthesis is an essential metabolic process and a validated target for the development of antibiotics.[3] Protein synthesis involves four consecutive phases—initiation, elongation, termination, and ribosome recycling. Of these phases, initiation of translation is the rate limiting and most highly regulated phase.[4] This critical step involves the formation of the 30S initiation complex (30S IC) and requires the three initiation factors: IF1, IF2, and

Grant sponsor: NIH; Grant number: 1SC3GM098173 (to J.B.); Grant sponsor: University of Texas – Pan American Faculty Research Council (FRC) award (to Y.Z.); Grant sponsor: University of Texas Rio Grande Valley Faculty Research Council (FRC) award (to Y.Z.); Grant sponsor: Welch Foundation (to UTRGV Chemistry Department); Grant number: BX-0048.

*Correspondence to: Yonghong Zhang, Chemistry Department, SCNE. 3.152, The University of Texas-RGV, 1201 W. University Drive, Edinburg, TX 785. E-mail: yonghong.zhang@utrgv.edu

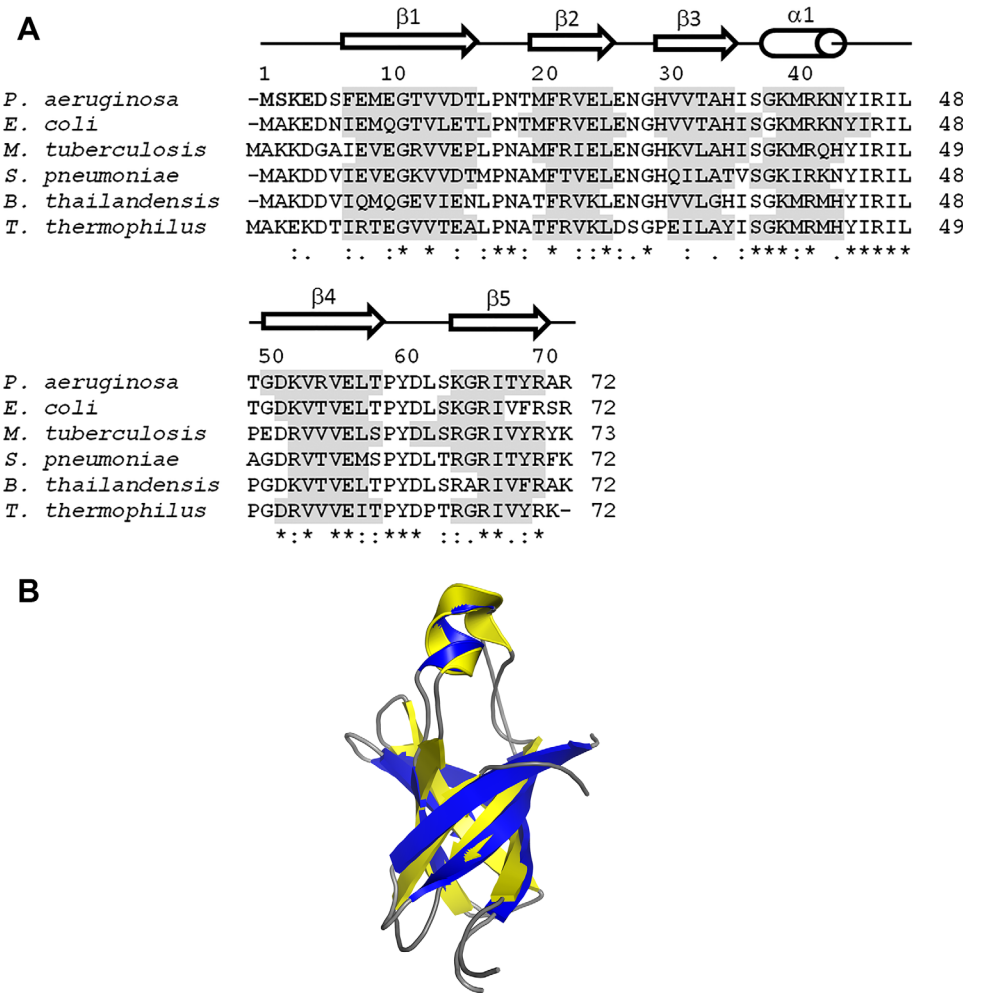

Figure 1. (A) Alignment (Clustal Omega) of the primary sequence of Pa-IF1 with those of other bacterial homologs from: *E. coli* (PDB 1AH9), *M. tuberculosis* (PDB 3I4O), *S. pneumoniae* (PDB 4QL5), *B. thailandensis* (PDB 2N3S), *T. thermophilus* (PDB 1HR0). Secondary structural elements, highlighted in gray, were derived from the PDB structures. The secondary structure elements of Pa-IF1 are indicated schematically above the sequence. (B) Overlay of Pa-IF1 (secondary structures in blue) and IF1 from *E. coli* (PDB 1AH9, secondary structures in yellow).

IF3. Prokaryotic protein synthesis in *Escherichia coli* (*E. coli*) has been well studied and recently the cryo-EM structure and real-time assembly landscape of the 30S IC have been determined.[5–8] To adapt this to drug discovery of new antimicrobial agents, atomic-level structural information will be required for the design and improvement of small-molecular inhibitors based on structure-activity relationship.

IF1 is the smallest of the three initiation factors and plays an important role in the initiation of protein synthesis by binding at the A-site of the 30S ribosomal subunit thereby preventing the initiator tRNA from binding at that site.[9] Several structures of bacterial IF1 in free form or bound to the 30S subunit have been reported including: *E coli* (PDB ID 1AH9),[7] *Mycobacterium tuberculosis* (PDB ID 3I4O),[8] and *Thermus thermophilus* (PDB ID 1HR0).[9] These structures are highly similar with respect to the oligonucleotide/oligosaccharide binding fold (OB fold); however, there are significant differences of the structure in the C-terminal region [Fig. 1(A)]. Several amino acids, especially Arg70 at the C-terminal end of IF1 from *E. coli* were identified as being critical for IF1 functionality.[7] However, these results are inconsistent with the crystal structure of IF1 bound to the 30S ribosomal subunit from *Thermus thermophilus* (PDB ID 1HR0). In this structure, the equivalent residue makes no direct contact with the 30S subunit, suggesting that IF1 from different species may exhibit distinct interaction with the 30S ribosomal subunit. In this study, we report the solution NMR structure of *P. aeruginosa* IF1 (Pa-IF1) at pH 5.1. We analyzed the conformational changes of *P. aeruginosa* IF1 in comparison with other bacterial IF1 structures, and propose the functional roles of conserved surface residues including the C-terminal end, which was disordered in the homologous structure.

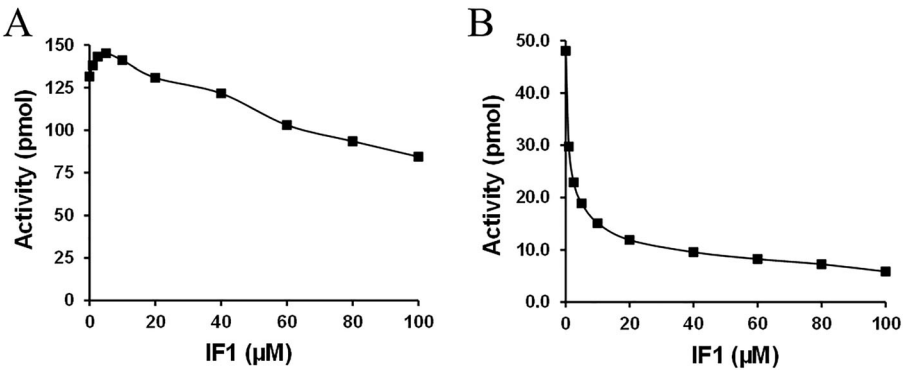

Figure 2. Characterization of *P. aeruginosa* IF1. (A) *P. aeruginosa* IF1 functions alone in the *P. aeruginosa* A/T assay to prevent formation of 70s ribosomes and, therefore, decreases poly-Phe synthesis; (B) IF1 enhances the inhibition of the formation of 70S ribosomes in the presence of 10 μ*M P. aeruginosa* IF3.

Results and Discussion

P. aeruginosa *IF1 expression and enzymatic characterization*

The gene (*inf*A) encoding IF1 from *P. aeruginosa* was cloned and fused to a downstream region encoding a hexahistidine tag. Over-expression of this construct yielded a small protein with a C-terminal hexahistidine tag with a molecular mass of 9.4 kDa. The resulting protein was expressed and purified to greater than 98% homogeneity. IF1 binds to the A site of the small subunit of the ribosome during initiation of protein synthesis preventing the initiator tRNA from binding that site, thus facilitating the formation of the 30S initiation complex. IF1 also aids in pre-mature formation of the 70S ribosome by preventing the binding of the 50S ribosomal subunit to the 30S initiation complex.[4,9,10] We hypothesized that we could use the *P. aeruginosa* aminoacylation/translation (A/T) assay[11,12] to detect the ability of Pa-IF1 in preventing association of the ribosomal subunits and, therefore, inhibit poly-Phe synthesis. When IF1 was titrated into the A/T assay alone, a modest inhibition of poly-Phe synthesis was observed [Fig. 2(A)]; however, when IF1 was titrated into the assay in the presence of 10 μ*M P. aeruginosa* IF3 (previously purified in our laboratory), a robust inhibition of poly-Phe synthesis resulted [Fig. 2(B)]. At lower concentrations (1, 2.5, 5, and 10 μ*M*) of IF1 alone, the poly-Phe product was slightly increased, which is consistent with previous results in which the initiation factors stimulate protein synthesis at low concentrations.[13] However, as the IF1 concentration was increased, poly-Phe synthesis decreased providing clear evidence that our hypothesis was correct and confirmed that IF1 was isolated in an active form. As can be seen in Figure 2(A,B), in the absence of IF1, poly-Phe synthesis is lower in the presence of IF3 than when IF3 is not present. This is accounted for by the fact that at 10 μ*M* IF3 also functions in the prevention of the formation of the 70s ribosome from its individual subunits during initiation of protein synthesis[14,15] thus reducing poly-Phe synthesis and as shown here IF1 enhances this activity.

NMR-derived structure of Pa-IF1

The ^{1}H-^{15}N heteronuclear single quantum correlation (HSQC) NMR spectrum of Pa-IF1 exhibited characteristics of a well-folded protein.[16] The spectrum was highly dispersed, and exhibited the expected number of backbone amide NMR cross peaks with uniform intensities and narrow peak shapes, indicating that the protein is monomeric, and adopts a stable three-dimensional structure. ^{15}N-NMR relaxation analysis (R_1 and R_2) of Pa-IF1 indicates an average rotational correlation time of ~5.8 ns (Fig. 3) and molecular weight of ~9 kDa, suggesting that Pa-IF1 forms a monomer under NMR conditions. NMR chemical shift assignments for Pa-IF1 were described previously[16] (BMRB no.

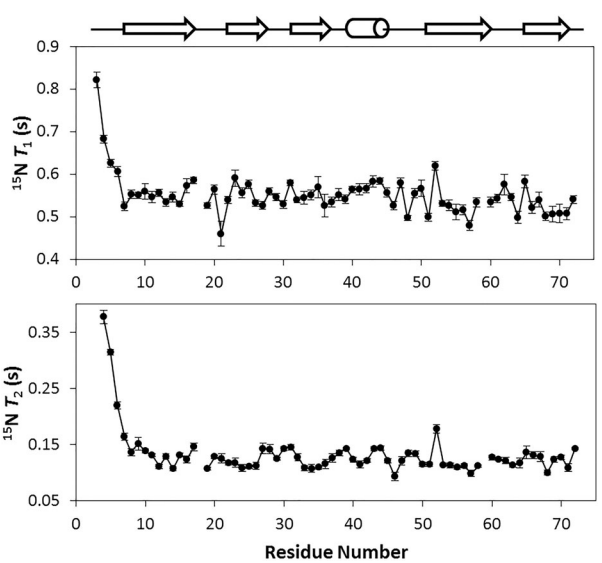

Figure 3. The NMR longitudinal relaxation (T_1) and transverse relaxation (T_2) of the residue-specific backbone amide ^{15}N of Pa-IF1 at 298 K. The secondary structure elements are indicated schematically at the top of the figure.

Table I. *Structure Calculation Statistics of NMR-Derived Structures of Pa-IF1*

NOE restraints (total)	620
Intra ($i-j=0$)	294
Medium ($1\leq i-j\leq 4$)	180
Long ($i-j>4$)	146
Dihedral angle restraints (φ and ψ)	122
Hydrogen bond restraints in β–strand regions	29
RMSD from ideal geometry	
Bond length (Å)	0.0099 ± 0.00018
Bond angles (deg)	2.02 ± 0.0122
Ramachandran plot	
Most favored region (%)	69.5
Allowed region (%)	29.5
Disallowed region (%)	1.0
RMSD from average structure	
β-barrel regions (main chain) (Å)	0.3 ± 0.089
β-barrel regions (non-hydrogen) (Å)	1.02 ± 0.10

26649). These assignments served as a basis for collecting nuclear Overhauser effect (NOE) distances, hydrogen-bonds, and dihedral angle restraints from the NMR experimental data used for the atomic-resolution structure calculation as described in the Methods section. Structural statistics for the 15 lowest energy conformers (Protein Data Bank accession no. 2N78) are summarized in Table I. The calculated structures were validated using PROCHECK, which shows that 99.0% of the residues belong to the most favorable/allowed region in the Ramachandran plot.

The final NMR-derived structures of Pa-IF1 are illustrated in Figure 4 and summarized in Table I. The 15 lowest energy conformers when superimposed have an overall main chain root mean square deviation (RMSD) of 0.3 Å [Fig. 4(A)]. The first six residues of the N-terminal end exhibit random-coil chemical shifts suggesting this region is disordered. However, the residues at the C-terminal end are well-defined and less flexible as supported by ^{15}N-{^{1}H} heteroNOEs.[16] The solution structure of Pa-IF1 consists of five-stranded β-sheet and one α-helix: β1 (residues 7–16), β2 (residues 21–26), β3 (residues 30–35), α1 (residues 38–43), β4 (residues 50–58), β5 (residues 64–70) [Fig. 4(B)]. The five strands are arranged in the sequential order β1-β2-β3-α1-β4-β5 as a β-barrel and oriented anti-parallel, except strands β3 and β5. While most of the turns between strands seem well defined as shown in Figure 4, the region connecting strands β3 and β4 (residues 36–49) appears to have considerable flexibility and contains a short α-helix (residues 38–43) as derived from medium-range NOEs supported by ^{15}N-{^{1}H} heteroNOEs.[16] The compact β-barrel is covered on one side by a long flexible loop. The Pa-IF1 adopts the expected OB fold indicative of its binding to the 30S ribosomal subunit.[17]

Surface properties of Pa-IF1

An electrostatic potential surface of Pa-IF1 [Fig. 4(C)] reveals that a surface composed of strands β4 and β5 located near the short α-helix is rich in basic residues (Arg and Lys), including K39, R41, K42, K64, R66, R70, and R72; while the other side is rich in acidic residues (Glu and Asp), such as E8, D15, E25, E27, and D51. We propose that the positively charged protein surface in Figure 4(C) may make contact with the 30S ribosomal subunit during binding. Indeed, these residues are conserved (K39, R41, R66, R70) or highly similar (K64 and R72) in all bacterial IF1 proteins, and have been shown to be involved in binding to the 30S ribosomal subunit in the crystal structure of IF1 from *Thermus thermophilus*.[9]

Structural comparison of bacterial IF1 proteins

There are several crystal or NMR structures of bacterial IF1 proteins available in the Protein Data Bank (http://www.pdb.org). Figure 1(A) shows the structure based sequence alignment of the known

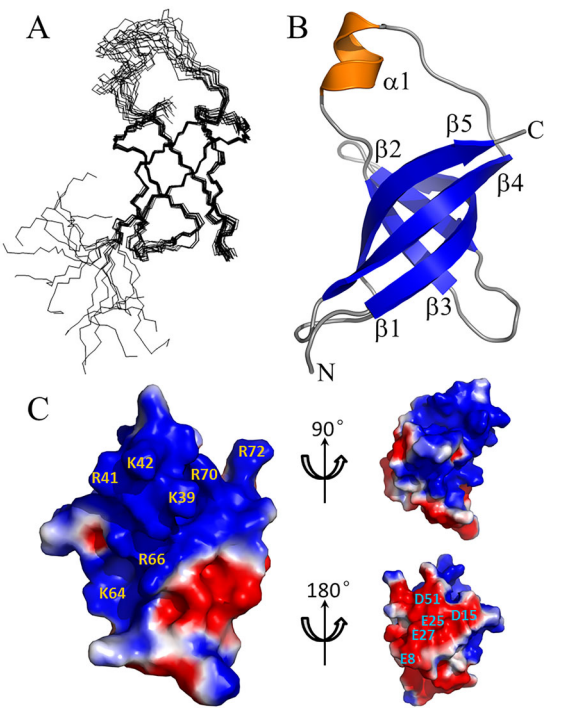

Figure 4. NMR-derived Structures of Pa-IF1. (A) Superposition of main chain atoms of 15-lowest-energy conformers with an RMSD of 0.3 Å (main chain atoms). The first six N-terminal residues are not folded in the structure. (B) Ribbon representation of the energy-minimized average main chain structure with secondary structures labeled (α-helix: orange; β strands: blue). (C) Surface presentation of the electrostatic potential (±1 kT/e) generated using the Adaptive Poisson-Boltzmann Equation (APBS) plugin in PyMOL with ionic strength 0.15 *M* and views at 90° and 180° rotation around the longitudinal axis. Red and blue colored regions denote negative and positive charges, respectively.

representatives of bacterial IF1. All of the IF1 homologs consist of five β-strands and one short α helix arranged as a compact β-barrel, and adopt an OB fold, indicating similar *in vivo* function. The amino acid sequence of Pa-IF1 is most similar to that of *E. coli* (86% identity) but also similar to that of *M. tuberculosis* (69%), *S. pneumoniae* (68%), *B. thailandensis* (67%), and *T. thermophilus* (56%). The main differences observed in the sequence alignments were in the non-conserved residues at the N- and C-terminal regions. Pa-IF1 has an extended β-strand at the C-terminus (β5), which is considerably rigid as indicated by ^{15}N-{^{1}H} heteroNOEs.[16] This is not the case for IF1 from *E. coli* which has a more flexible C-terminal end as shown in Figure 1(B). Interestingly, the Pa-IF1 C-terminus region is more similar to that of the more recently solved structure of *S. pneumoniae* IF1 (PDB 4QL5) in sequence and structure although they share less sequence identity (68%). The residues at the C-terminal end (e.g., R70) have previously been shown to be critical for IF1 functionality.[18] The structural differences suggest that IF1 from different species may exhibit distinct interaction with their cognate 30S ribosomal subunit.

Methods

Materials

Oligonucleotides were from Integrated DNA Technologies (Coralville, IA). All other chemicals were obtained from Fisher Scientific (Pittsburg, PA). DNA sequencing was by Functional Bioscience (Madison, WI). Radioactive isotopes were from PerkinElmer (Waltham, MA).

Preparation of P. aeruginosa *IF1*

The gene encoding IF1 was amplified by PCR (Bio-Rad MJ Mini Thermo Cycler) from *P. aeruginosa* PAO1 (ATCC 47085) genomic DNA using the forward primer (5′-ttccgctagcaaagaagacagcttcgaaatgg-3′) which added an *Nhe*I restriction site to the 5′ end of the gene and the reverse primer (5′-taatctcgaggcgggcgcggtaggt-3′) which added an *Xho*I restriction site to the 3′ end of the gene. The PCR product was inserted into a pET-24b(+) plasmid (Novagen) digested with *Nhe*I/*Xho*I placing the gene upstream of a sequence encoding six histidine residues. The recombinant plasmid was subsequently transformed into Rosetta 2(DE3) competent cells (Novagen).

To produce IF1 for use in structural studies, ^{15}N-labeled or ^{13}C/^{15}N-labeled Pa-IF1 was prepared using the high cell density method.[19] The protein was concentrated and the buffer was changed to 100 m*M* KCl and 20 m*M* KH_2PO_4 (pH 5.1) using Amicon Ultra-15 Centrifugal Filters (EMD Millipore).

To prepare IF1 for functional studies, the bacterial was grown using Terrific Broth, harvested and Fraction 1 lysate was prepared and the protein isolated as described.[20] *P. aeruginosa* IF1 was initially purified by precipitation between 30% and 70% saturated ammonium sulfate and further purified using nickel-nitrilotriacetic acid affinity chromatography (Perfect Pro, 5 Prime). The protein was then dialyzed (two times) against a buffer containing 20 m*M* Hepes-KOH (pH 7.0), 40 m*M* KCl, 1 m*M* $MgCl_2$, 0.1 m*M* EDTA, 10% glycerol, aliquoted, and fast frozen in liquid nitrogen and stored at −80°C.

P. aeruginosa *IF1 assays*

IF1 was analyzed for its ability to inhibit poly-Phe synthesis in the *P. aeruginosa* A/T assays by preventing association of the ribosomal subunits. In addition to the A/T assay components, the reactions contained IF1 at varying concentrations (0, 1, 2.5, 5, 10, 20, 40, 60, 80, and 100 μ*M*) in the presence or absence of IF3 (10 μ*M*). The reactions (50 μL) were carried out in 96 well microtiter plates (Costar) at ambient temperature for 60 min. Reactions were stopped by the addition of 5 μL of 0.5 *M* EDTA and analyzed using scintillation proximity assay technology.[21]

NMR spectroscopy

NMR samples of Pa-IF1 (∼1.0 m*M*, unlabeled, ^{15}N- or ^{15}N/^{13}C-labeled) were prepared in 90%/10% H_2O/D_2O or 100% D_2O with 20 m*M* phosphate (pH 5.1), 100 m*M* KCl. A D_2O-exchanged sample was prepared for H-D exchange experiments by freezing the Pa-IF1 sample followed by lyophilization and resuspension in 99.9% D_2O. All NMR experiments were performed at 298 K on a Bruker AVANCE III Ultrashield Plus 600 MHz spectrometer equipped with a double resonance broad band room-temperature probe (BBO), or a Bruker AVANCE 700 MHz or 600 MHz spectrometer both equipped with a four channel interface and triple resonance cryogenic probe (TXI) with triple-axis (*X*,*Y*,*Z*) pulsed field gradients. Backbone and side-chain NMR chemical shift assignments were obtained by analyzing the following spectra: HNCACB, CBCA(CO)NH, HNCO, HBHA(CO)NH, and ^{15}N-HSQC-TOCSY (mixing time of 60 ms) spectra. The additional side-chain aliphatic ^{1}H and ^{13}C resonances were assigned using ^{13}C-CT-HSQC, ^{13}C-HCCH-TOCSY, and CCH-TOCSY spectra. For aromatic side-chain chemical shift assignments, ^{13}C-CT-HSQC-TOCSY, ^{13}C-HSQC-NOESY (mixing time of 120 ms) spectra along with 2D ^{1}H-^{1}H NOESY (mixing time of 100 ms), and TOCSY (mixing time of 100 ms), were used. Stereospecific assignments of chiral methyl groups of valine and leucine were obtained by analyzing ^{1}H-^{13}C HSQC experiments performed on a sample that contained 10% ^{13}C labeling of IF1.[22] For ^{15}N relaxation experiments, the longitudinal magnetization (T_1) decay was recorded at six different times: 0.00, 0.10, 0.25,

0.50, 1.00, and 2.00 s. The transverse magnetization (T_2) decay was recorded with eight different delays: 0.000, 0.008, 0.016, 0.032, 0.048, 0.080, 0.120, and 0.200 s. To check the sample stability the transverse magnetization decay at 0.016 s was verified to be unchanged before and after each set of measurements of both ^{15}N T_1 and T_2 experiments. The T_1 and T_2 data were fitted to a single exponential decay function, $I = I_0 e^{-t/Td}$, in which I is the signal intensity at time t, I_0 is the intensity at $t = 0$, and Td is the decay constant T_1 and T_2, respectively. The NMR data were processed using NMRPipe (http://spin.niddk.nih.gov/NMRPipe/) and analyzed using Sparky (University of California, San Francisco).

NMR structural calculation

NOE-based inter-proton distance restraints were collected through analysis of NOESY data. The NMR-derived distance, hydrogen bond distance and dihedral angles (ϕ and φ) generated by TALOS then served as restraints (see Table I) for calculating the three dimensional structure of Pa-IF1 using distance geometry and restrained molecular dynamics. Structure calculations were performed by Xplor-NIH 2.38 using a simulated annealing protocol.[23] A total of 620 inter-proton distance restraints were obtained by analysis of ^{15}N-edited and ^{13}C-edited 3D NOESY-HSQC and 2D ^{1}H-^{1}H NOESY spectra. In addition to the NOE-derived distance restraints, the following additional restraints were included in the structure calculation: 122 dihedral angle restraints (φ and ψ); 29 hydrogen bonds verified by identifying slowly exchanging amide protons in hydrogen-deuterium exchange experiments. Fifty independent structures were calculated, and after refinement, the 15 structures of lowest energy were selected and analyzed. The average total and experimental distance energy were 1883 ± 21 and 215 kcal mol^{-1}. The average root-mean-square deviation from an idealized geometry for bonds and angles were 0.0099 Å and 2.02°. The NMR-derived structures of Pa-IF1 were assessed by PRO-CHECK. The final NMR ensemble of 15 structures with the lowest energy has been deposited in the RCSB Protein Data Bank (PDB ID 2N78).

Acknowledgments

Authors thank Drs. Andrew P. Hinck and Kristin E. Cano-McCue for technical support and help with NMR experiments at UTHSCSA, and Mr. Thomas Eubanks for NMR technical support at UTRGV. Disclosure: All authors declare no conflict of interest.

References

1. Stover CK, Pham XQ, Erwin AL, Mizoguchi SD, Warrener P, Hickey MJ, Brinkman FS, Hufnagle WO, Kowalik DJ, Lagrou M, Garber RL, Goltry L, Tolentino E, Westbrock-Wadman S, Yuan Y, Brody LL, Coulter SN, Folger KR, Kas A, Larbig K, Lim R, Smith K, Spencer D, Wong GK, Wu Z, Paulsen IT, Reizer J, Saier MH, Hancock RE, Lory S, Olson MV (2000) Complete genome sequence of *Pseudomonas aeruginosa* PAO1, an opportunistic pathogen. Nature 406:959–964.
2. Hirsch EB, Tam VH (2010) Impact of multidrug-resistant *Pseudomonas aeruginosa* infection on patient outcomes. Expert Rev Pharmacoecon Outcomes Res 10: 441–451.
3. McCoy LS, Xie Y, Tor Y (2011) Antibiotics that target protein synthesis. RNA 2:209–232.
4. Laursen BS, Sorensen HP, Mortensen KK, Sperling-Petersen HU (2005) Initiation of protein synthesis in bacteria. Microbiol Mol Biol Rev 69:101–123.
5. Julian P, Milon P, Agirrezabala X, Lasso G, Gil D, Rodnina MV, Valle M (2011) The cryo-EM structure of a complete 30S translation initiation complex from *Escherichia coli*. PLoS Biol 9:e1001095.
6. Milon P, Maracci C, Filonava L, Gualerzi CO, Rodnina MV (2012) Real-time assembly landscape of bacterial 30S translation initiation complex. Nat Struct Mol Biol 19:609–615.
7. Sette M, van Tilborg P, Spurio R, Kaptein R, Paci M, Gualerzi CO, Boelens R (1997) The structure of the translational initiation factor IF1 from *E. coli* contains an oligomer-binding motif. EMBO J 16:1436–1443.
8. Hatzopoulos GN, Mueller-Dieckmann J (2010) Structure of translation initiation factor 1 from *Mycobacterium tuberculosis* and inferred binding to the 30S ribosomal subunit. FEBS Lett 584:1011–1015.
9. Carter AP, Clemons WM Jr, Brodersen DE, Morgan-Warren RJ, Hartsch T, Wimberly BT, Ramakrishnan V (2001) Crystal structure of an initiation factor bound to the 30S ribosomal subunit. Science 291:498–501.
10. Dahlquist KD, Puglisi JD (2000) Interaction of translation initiation factor IF1 with the *E. coli* ribosomal A site. J Mol Biol 299:15.
11. Ribble W, Hill WE, Ochsner UA, Jarvis TC, Guiles JW, Janjic N, Bullard JM (2010) Discovery and analysis of 4H-pyridopyrimidines, a class of selective bacterial protein synthesis inhibitors. Antimicrob Agents Chemother 54:4648–4657.
12. Hu Y, Palmer SO, Keniry M, Bullard JM (2016) Discovery and analysis of natural product compounds inhibiting protein synthesis in *Pseudomonas aeruginosa*. Antimicrob Agents Chemother 60:4820–4829.
13. Wahba AJ, Iwasaki K, Miller MJ, Sabol S, Sillero MA, Vasquez C (1969) Initiation of protein synthesis in *Escherichia coli*. II. Role of the initiation factors in polypeptide synthesis. Cold Spring Harb Symp Quant Biol 34:291–299.
14. Petrelli D, LaTeana A, Garofalo C, Spurio R, Pon CL, Gualerzi CO (2001) Translation initiation factor IF3: two domains, five functions, one mechanism? EMBO J 20:4560–4569.
15. MacDougall DD, Gonzalez RL Jr (2015) Translation initiation factor 3 regulates switching between different modes of ribosomal subunit joining. J Mol Biol 427: 1801–1818.
16. Bernal A, Hu Y, Palmer SO, Silva A, Bullard JM, Zhang Y (2016) ^{1}H, ^{13}C and ^{15}N resonance assignments and secondary structure analysis of translation initiation factor 1 from *Pseudomonas aeruginosa*. Biomol NMR Assign. DOI 10.1007/s12104-016-9678-7
17. Murzin AG (1993) OB(oligonucleotide/oligosaccharide binding)-fold: common structural and functional solution for non-homologous sequences. EMBO J 12:861–867.

18. Spurio R, Paci M, Pawlik RT, La Teana A, Di Giacco BV, Pon CL, Gualerzi CO (1991) Site-directed mutagenesis and NMR spectroscopic approaches to the elucidation of the structure-function relationships in translation initiation factors IF1 and IF3. Biochimie 73:1001–1006.
19. Sivashanmugam A, Murray V, Cui C, Zhang Y, Wang J, Li Q (2009) Practical protocols for production of very high yields of recombinant proteins using *Escherichia coli*. Protein Sci 18:936–948.
20. Cull MG, McHenry CS (1995) Purification of *Escherichia coli* DNA polymerase III holoenzyme. Methods Enzymol 262:22–35.
21. Macarron R, Mensah L, Cid C, Carranza C, Benson N, Pope AJ, Díez E (2000) A homogeneous method to measure aminoacyl-tRNA synthetase aminoacylation activity using scintillation proximity assay technology. Anal Biochem 10:183–190.
22. Neri D, Szyperski T, Otting G, Senn H, Wüthrich K (1989) Stereospecific nuclear magnetic resonance assignments of the methyl groups of valine and leucine in the DNA-binding domain of the 434 repressor by biosynthetically directed fractional 13C labeling. Biochemistry 28:7510–7516.
23. Nilges M, Gronenborn AM, Brunger AT, Clore GM (1988) Determination of three-dimensional structures of proteins by simulated annealing with interproton distance restraints. Application to carmbin, potato carboxypeptidase inhibitor and barley serine proteinase inhibitor 2. Protein Eng 2:27–38.